Aberystwyth University

Isochron dating of sediments using luminescence of K-feldspar grains
Li, Bo; Li, Sheng-Hua; Wintle, Ann G.; Zhao, Hui

Isochron dating of sediments using luminescence of K-feldspar grains

Bo Li,[1] Sheng-Hua Li,[1] Ann G. Wintle,[2] and Hui Zhao[3]

[1] A new method for dating well-bleached sediments is presented, with results for thirteen samples from China. The method uses an isochron constructed from the measurement of natural radiation doses received by potassium-feldspar grains in a range of grain sizes using the infrared stimulated luminescence (IRSL) signal. The age of deposition of the sediment is calculated from this isochron and from the internal dose rate to the grains from ^{40}K and ^{87}Rb in the crystal lattice. This procedure appears to overcome age underestimation due to anomalous fading, a phenomenon that has precluded conventional luminescence dating of K-feldspars and would be applicable to K-feldspars for which the natural dose is beyond the linear dose response region. Also, since the isochron IRSL method is reliant on only the internal dose rate, it overcomes problems related to (1) changes in past dose rate due to postdepositional migration of radionuclides, (2) changes in water content as water-lain sediments dry out, (3) spatial heterogeneity in the gamma dose rate, and (4) uncertainties in the cosmic ray dose rate during the period of sample burial.

1. Introduction

[2] Sedimentary deposits such as the desert sands of northeastern China provide a record of past climate change. The record is particularly sensitive to climate change in the transition zone between the desert and loess areas at the southern edge of the Mu Us desert; this transition zone responds to changes in the east Asia monsoonal circulations [*Sun et al.*, 1999]. In order to investigate these changes, it is imperative to obtain a chronological framework. This study was aimed at the development of such a framework for this climatically sensitive region, but the method presented could be used anywhere in the world where the sediments contain well-bleached potassium feldspar grains in a range of grain sizes.

[3] Dating of sedimentary deposits can be achieved using luminescence techniques [*Aitken*, 1985, 1998] in which the luminescence signals of grains of quartz or feldspar are used to measure the dose received by the grains in their sedimentary environment since deposition. This dose is termed the equivalent dose, D_e. In standard luminescence dating techniques, the age is obtained by dividing the D_e (in Gy) by the dose rate (Gy/ka) which is made up of two contributions, the external dose rate and the internal dose rate. The external dose rate is derived from the decay of radio-

nuclides, and a contribution from cosmic rays, outside the grain and is calculated from measurements of the radionuclides contained in the bulk sediment [*Aitken*, 1985] and the cosmic ray flux [*Prescott and Hutton*, 1994]. The internal dose rate is derived from radionuclides within the grains; in the case of sand-sized grains of alkali feldspars (K-feldspars), this dose is mainly due to ^{40}K and ^{87}Rb found within the crystal lattice.

[4] An early attempt to provide a chronology for the sand/loess/palaeosol records in this area was carried out using the thermoluminescence (TL) [*Aitken*, 1985] signals from polymineral silt-sized grains [*Sun et al.*, 1998]. The ages obtained for the last glacial/interglacial cycle were stratigraphically consistent. In more recent studies, the more light-sensitive optically stimulated luminescence (OSL) [*Aitken*, 1998] signals from chemically isolated quartz grains have been used [*Li and Sun*, 2006; *Li et al.*, 2002]; this signal is more rapidly and more completely zeroed than the TL signal of quartz and feldspars. For Holocene deposits, OSL dating has been applied to quartz grains from the fossil dunes in the Hulun Buir Desert [*Li and Sun*, 2006] and the Hunshundake Desert [*Li et al.*, 2002], north of Beijing. However, the dating of earlier deposits is limited by the saturation of the quartz OSL signal with increasing dose [*Bøtter-Jensen et al.*, 2003].

[5] Besides giving an OSL signal when stimulated at visible wavelengths, feldspars also give a luminescence signal when the grains are stimulated at wavelengths around 800–900 nm [*Bøtter-Jensen et al.*, 2003]; this is termed infrared stimulated luminescence (IRSL). The IRSL signal from K-feldspars has many advantages over the OSL signal of quartz. In the context of extending the time frame for sedimentary deposits, it has been found that the IRSL signal from sand-sized K-feldspar grains does not saturate until

---

[1]Department of Earth Sciences, The University of Hong Kong, Hong Kong.
[2]Institute of Geography and Earth Sciences, University of Wales Aberystwyth, Aberystwyth, UK.
[3]Key Laboratory of Desert and Desertification, Cold and Arid Regions Environment and Engineering Research Institute, Chinese Academy of Sciences, Lanzhou, China.

much higher doses are reached. In addition, the IRSL signal is bright compared with the quartz OSL signal, partly due to the much wider optical detection window that can be used when stimulating in the infrared. This enables high-precision luminescence measurements to be made, which generally leads to high reproducibility for the natural dose measurements [*S.-H. Li et al.*, 2007]. The high contribution of ^{40}K and ^{87}Rb to the internal dose rate will create more luminescence, which generally results in more precise values of the measured equivalent dose for young samples. The higher internal dose rate will also reduce the effect on the total dose rate of inhomogeneity in the external dose rate, again resulting in higher precision. However, dating using the IRSL signal from sand-sized K-feldspar grains has not been adopted widely mainly because the IRSL ages are underestimated when compared with independent age control or ages derived from OSL measurements of quartz [*Wallinga et al.*, 2001].

[6] K-feldspars have long been known to exhibit anomalous fading of their luminescence signals when measured following laboratory irradiation [*Wintle*, 1973]. In particular, IRSL signals have been shown to decrease with storage at room temperature, even though the relevant electron traps should be thermally stable for geologically long periods of time (hence the use of the term "anomalous" to describe the observed fading) [*Huntley and Lamothe*, 2001; *Huntley and Lian*, 2006; *Spooner*, 1992, 1994]. Several methods have been proposed to measure the decay over periods of time up to 1 year [*Auclair et al.*, 2003; *Huntley and Lamothe*, 2001] and the fading appears to follow a power law with linear decay on a log (time) scale. This enables the calculation of a fading rate (*g* value) in terms of percent loss per decade, where a decade is a factor of 10 in time since laboratory irradiation [*Aitken*, 1985]. *Huntley and Lian* [2006] measured *g* values of 3–7% per time decade for most of the 77 samples of K-feldspars that they extracted from sediments from around the world.

[7] In a study of K-feldspars from three samples of desert sand from northeast China, *B. Li et al.* [2007] found fading rates of between 2 and 4% per decade when they applied the fading measurement procedure recommended by *Auclair et al.* [2003]. *B. Li et al.* [2007] also found the fading rates of laboratory-irradiated samples to be independent of grain size, when sand-sized K-feldspar grains of between 90 and 250 μm in diameter were measured. However, when they measured the equivalent doses for each of these grain sizes (90–125, 125–150, 150–180, 180–212, and 212–250 μm) and used the internal beta dose rate together with the measured environmental dose rate for each sample, they observed that there was an upward trend in IRSL age with increasing grain size. This implied that, in the natural environment, the fading rates of different grain sizes were actually different. Their data led *B. Li et al.* [2007] to conclude that only that part of the signal induced by the external dose rate suffers from fading, which explains why fading is ubiquitous for samples irradiated in the laboratory. Comparison of the ages for these K-feldspar grains derived using the internal dose rate appropriate for each grain size and the OSL ages obtained from quartz grains of a matching size led *B. Li et al.* [2007] to conclude that that part of the IRSL signal resulting from the internal dose rate had not faded in the natural environment.

[8] In this paper we propose an isochron dating method for K-feldspars that utilizes this conclusion; this new method is termed the isochron IRSL method to distinguish it from previous isochon methods that employ measurement of quartz grains in addition to K-feldspars [*Zhao and Li*, 2002; *B. Li et al.*, 2007]. In addition, since this procedure relies solely on the value of the internal dose rate (derived from ^{40}K and ^{87}Rb), it can also be used to derive ages for samples for which there have been past changes in the external dose rate. Experimental data will be presented for K-feldspar grains that have given underestimation of D_e, and thus age, when using conventional IRSL dating procedures either due to anomalous fading or due to changes in dose rate, but which yield correct ages using the isochron IRSL approach. Furthermore, the isochron IRSL method avoids having to make corrections to the IRSL data using the laboratory-measured *g* value [*Huntley and Lamothe*, 2001] required for even relatively young samples [e.g., *Wolfe et al.*, 2006]. It also avoids having to attempt fading corrections for older samples [*Lamothe and Auclair*, 1999; *Lamothe et al.*, 2003], since it has been shown that there is a complex relationship between the *g* value and the age of samples buried for long enough to fill all available electron traps [*Huntley and Lian*, 2006].

2. Study Sites and Sample Locations

[9] The sedimentary samples used in this study are from four different deserts from Northern China, namely the Mu Us, Horqin, Hulun Buir, and Hunshandake. Figure 1 shows the location of the deserts and the sampling sites. Deposits in these desert areas contain little organic material that would enable radiocarbon dating to be applied. Thus, it has not been possible to obtain samples with tight age constraints using an independent radiometric method. However, we have measured OSL ages for quartz grains for a number of these samples and also have some age control from the stratigraphy as discussed below.

[10] Samples Sm1, Sm2, Sm3, Sm4, Sm0404, and Sm5 are aeolian sediments taken from Shimao section in the transition zone between the Mu Us Desert and the Loess plateau (Figure 1). The section contains sand beds, loess layers and palaeosols, which can be correlated with the deep-sea oxygen isotope stages (OIS) [*Sun et al.*, 1999, 1998]. The detailed stratigraphy of the section and previous TL ages have been reported elsewhere [*Sun et al.*, 1999, 1998]. Figure 2 shows the stratigraphy, magnetic susceptibility curve of the Shimao section and the sampling positions of Sm1, Sm2, Sm3 Sm4, Sm0404, and Sm5. For comparison, the marine oxygen isotope curve (SPECMAP) [*Imbrie et al.*, 1984] is also shown (redrawn from *Sun et al.* [1998]). Samples Sm1 and Sm2 were collected from the upper and lower part of the sand layer L1–1 immediately below the Holocene soil layer S0. Samples Sm3 and Sm4 were collected from layers L1–3 and L1–5, corresponding to OIS 3; thus the expected ages are between 59 and 29 ka [*Thompson and Goldstein*, 2006; *Voelker*, 2002], provided that there are no significant lags between the marine and terrestrial records. Quartz OSL ages for samples Sm1, Sm2, Sm3, and Sm4 were obtained in the course of this study (Table 1). Sample Sm0404 was taken from the boundary of
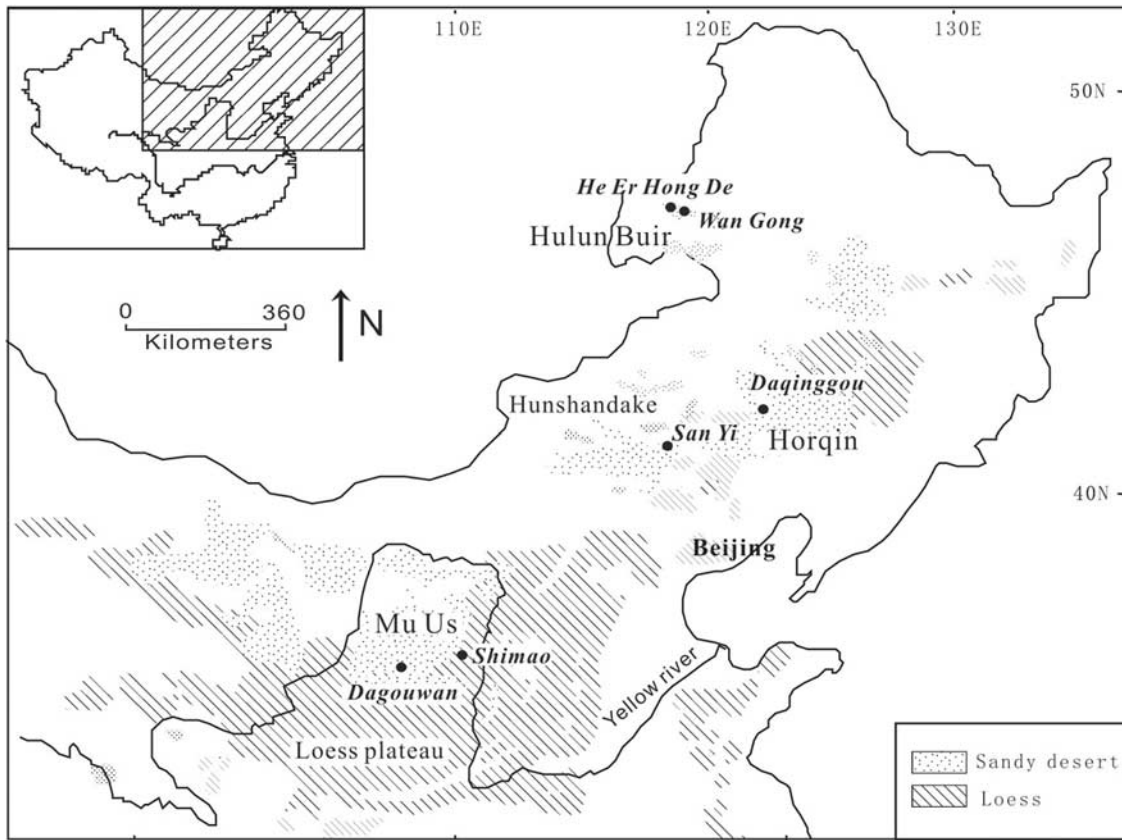
Figure 1. Deserts in northern China and sampling sites. Solid circles are the sampling locations with names shown in italics.
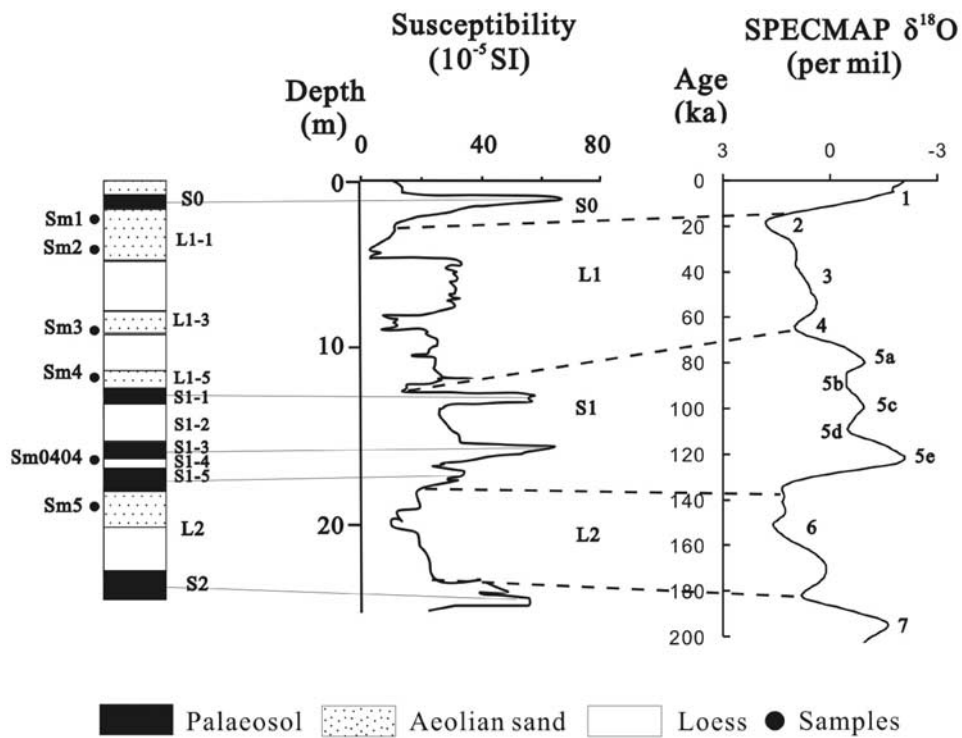

Figure 2. Stratigraphy, sampling positions, and magnetic susceptibility curve of the Shimao section and the marine oxygen isotope curve (SPECMAP) on its own timescale [*Imbrie et al.*, 1984]. This figure is modified from *Sun et al.* [1998].

Table 1. Summary of Age Estimates, *g* Values, and External Dose Rates

Sample	Independent Age[a] (ka)	Isochron IRSL Age (ka)	K-Feldspar Conventional IRSL Age[b] (ka)	Fading-Corrected Conventional IRSL Age (ka)	*g* Value[c] (%/decade)	External Dose Rate[d] (Gy/ka)
D4	3.0 ± 0.2	2.8 ± 0.5	2.8 ± 0.1		-	4.9 ± 0.2
WG3	13.2 ± 0.8	12.2 ± 2.3	8.9 ± 0.5	13.4 ± 0.8	3.4 ± 0.6	3.7 ± 0.2
HLD3	10.8 ± 1.2	10.4 ± 2.6	9.0 ± 0.4	12.4 ± 0.4	3.2 ± 0.3	2.9 ± 0.1
SY3	11.1 ± 1.3	10.9 ± 1.5	8.4 ± 0.4	11.2 ± 0.6	3.0 ± 0.6	3.1 ± 0.2
Dgw3	8.3 ± 0.5	7.8 ± 3.6	-		-	-
Dgw4	8.3 ± 0.5	8.5 ± 1.0	-		-	-
Dgw5	8.3 ± 0.3	8.7 ± 1.5	8.9 ± 0.3	11.4 ± 0.6	2.6 ± 0.5	2.6 ± 0.1
Sm1	9.1 ± 0.5	10.9 ± 1.5	8.5 ± 0.4	11.7 ± 0.5	3.2 ± 0.4	3.3 ± 0.2
Sm2	9.2 ± 0.3	8.5 ± 1.2	9.0 ± 0.5	12.7 ± 0.8	3.4 ± 0.6	3.2 ± 0.1
Sm3	40 ± 4	41 ± 6	37 ± 2	54 ± 3	3.3 ± 0.5	3.1 ± 0.1
Sm4	40 ± 3	40 ± 6	38 ± 2	53 ± 3	3.1 ± 0.5	3.0 ± 0.1
Sm0404	104−110	92 ± 20	57 ± 2	>78 ± 3	2.8 ± 0.3	3.6 ± 0.2
Sm5	125−140	121 ± 26	70 ± 3	>90 ± 4	3.2 ± 0.2	3.2 ± 0.1

　　[a]For samples Dgw3 and Dgw4, the environmental dose rates had changed significantly during burial time [see *Li et al.*, 2008] and thus reliable quartz OSL ages and feldspar IRSL ages could not be calculated; the ages shown for these are based on the stratigraphic evidence. For samples Sm0404 and Sm5, the ages shown are expected ages obtained by correlation with the SPECMAP timescale; dating with quartz was problematic because of the saturation of the fast component at the high environmental dose rates (>3.0 Gy/ka). For the other samples, the ages are based on quartz OSL ages obtained from grains of 125−150 μm in diameter.
　　[b]The conventional K-feldspar IRSL ages listed are based on grains of 125−150 μm in diameter.
　　[c]The *g* values shown are corresponding to a starting time of the first measurement (t_c) of 430 s.
　　[d]The dose rates were obtained using the dose rate conversion factors of *Adamiec and Aitken* [1998] together with measurements of current environmental radioactivity.

the soil layers S1−3 and S1−4, corresponding to the boundary of OIS 5c and 5d (OIS 5.4 and OIS 5.33), respectively; thus the expected age is between 110.1 and 104 ka [*Thompson and Goldstein*, 2006]. Sample Sm5 was taken from the upper part of L2, corresponding to OIS 6.0; thus the expected age is between 140 and 125 ka. No OSL ages were able to be obtained on the quartz grains from Sm0404 and Sm5 as the fast component OSL signal was saturated. The age ranges for Sm0404 and Sm5 given in Table 1 as evidence of independent age are based on the stratigraphic evidence.

[11] Quartz OSL ages are also presented in Table 1 for the other aeolian samples from the Hulun Buir, Hunshandake, and Horquin desert areas. WG3 (from Wan Gong in the Hulun Buir Desert), HLD3 (from He Er Hong De in the Hulun Buir Desert) and SY3 (from San Yi in the Hunshandake Desert) have quartz OSL ages of 10−13 ka (Table 1) that are in agreement with geological expectation [*Li and Sun*, 2006; *Li et al.*, 2002]. Sample D4 (from Daqinggou, Horqin Desert) has a quartz OSL age of 3.0 ± 0.2 ka [*Zhao and Li*, 2002].

[12] Waterlain deposits from the Dagouwan section of the Sala Us (Salawusu) River in the Mu Us desert (Figure 1) (Dgw3, Dgw4, and Dgw5) were also investigated. A detailed description of the Dagouwan section has been given by *Sun* [2000]. Samples Dgw3, Dgw4, and Dgw5 were located in Holocene lacustrine and fluvial sediment layers [*Li et al.*, 2008]. The middle and bottom of the

Holocene layer yielded ^{14}C ages of 5070 ± 70 and 9510 ± 110 a B.P. (where a is years), respectively [*Li et al.*, 1984; *Sun*, 2000], equivalent to calendar year ages of BC 3875 ± 78 and BC 9057 ± 73 [*Reimer et al.*, 2004], respectively; however, this provided only limited age control. The grains in these lacustrine and fluvial sediments, underlying the modern dune sands, were originally derived from aeolian sand and have been reworked by water and deposited as lake and river sediments. The samples in the current study, Dgw3, Dgw4, and Dgw5, were located between the stratigraphic positions of the samples giving the two ^{14}C ages. Better control is provided by the quartz OSL ages [*Li et al.*, 2008]. Sample Dgw5, which (at a depth of 1.35 m) overlay samples Dgw4 (1.55 m) and Dgw3 (1.75 m), gave a quartz OSL age of 8.3 ± 0.3 ka and an aeolian sand sample Dgw1 at 2.5 m depth (0.75 m beneath Dgw3) gave a quartz OSL age of 8.4 ± 0.3 ka [*Li et al.*, 2008]. Thus, both Dgw3 and Dgw4 are expected to be 8.3 ± 0.5 ka in age (Table 1). However, for these samples, the present-day environmental dose rates (calculated using the conversion factors of *Adamiec and Aitken* [1998]) are almost twice those of the six overlying samples (including Dgw5) and the underlying sample (Dgw1); thus there appears to have been a significant change in the concentrations of radioactive elements and a likely associated variation in the water content [*Li et al.*, 2008]. Thus the quartz OSL ages and feldspar IRSL ages for Dgw3 and Dgw4 calculated using the present-day dose rates were not in stratigraphic order [*Li et al.*, 2008]

Table 2. K Contents of K-Feldspar Fractions for Different Grain Sizes[a]

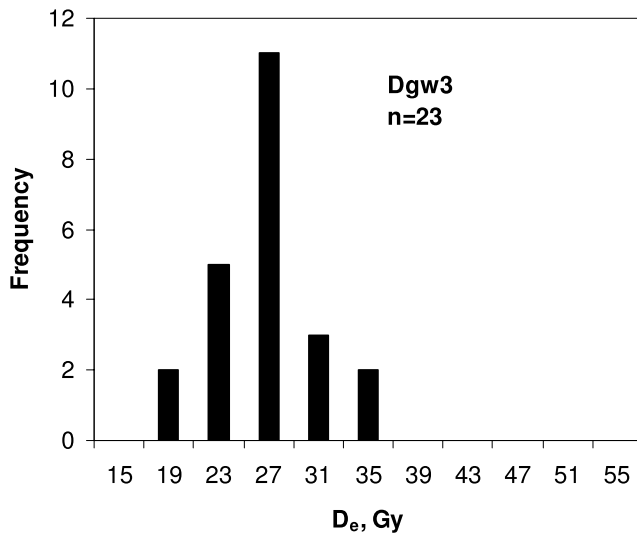| Sample	90−125 μm	125−150 μm	150−180 μm	180−212 μm	212−250 μm
Sm1	11.4 ± 0.6	13.3 ± 1.0	12.2 ± 0.6	14.3 ± 1.0	14.2 ± 0.7
SY3	11.6 ± 0.8	13.8 ± 1.0	13.3 ± 1.0	14.0 ± 1.0	12.9 ± 0.9
HLD3	-	10.2 ± 0.7	11.2 ± 0.8	12.2 ± 0.8	11.9 ± 0.9

　　[a]K contents are given in percents.

Figure 3. Histogram of quartz OSL D_e values from 125 to 150 μm grains from sample Dgw3.

and cannot be used to provide direct age constraint.

[13] The sediments listed above were chosen as they contain a wide range of grain sizes, thus making them suitable for the new method. Although a poorly sorted deposit may be interpreted as resulting from the transport of sediment over short distances, OSL measurements of quartz grains from modern dune sands in the deserts of northern China gave very young ages (<100 years) [Li et al., 2002], suggesting that the aeolian sediments in this study were well bleached before deposition. However, the Dagouwan samples (Dgw3, Dgw4, and Dgw5) were from lacustrine deposits. To test whether the sand-sized grains were well bleached prior to burial, 23 small aliquots of quartz containing ~100 grains of 125–150 μm were measured. Figure 3 shows the histogram of the distribution of D_e values for sample Dgw3. The absence of a long tail in the D_e distribution and its normal shape (Figure 3) suggests that the samples were well bleached and thus are appropriate for the isochron IRSL method.

3. Experimental Procedures

[14] The K-feldspar grains were extracted using standard preparation methods (for details see B. Li et al. [2007]) with at least four of the following grain size fractions being prepared for each sample (63–90, 90–125, 125–150, 150–180, 180–212, and 212–250 μm). The K-feldspar grains were etched using 10% HF for 40 min to remove the alpha irradiated surface of the grains.

[15] Quartz grains of 125–150 μm diameter were also extracted for comparison; these were etched with 40% HF for 40 min. Their OSL signals were measured on a Risø TL-DA-15 reader equipped with blue LEDs for stimulation [Bøtter-Jensen et al., 2003]. The OSL signal was measured at 125°C for 100 s and was detected using a photomultiplier tube with the OSL signal passing through 7.5 mm of U-340 filter. The quartz D_e values were determined using a single-aliquot regenerative dose (SAR) protocol [Murray and Wintle, 2000] with a preheat temper-

ature of 260°C (held for 10 s) for the natural and regenerative doses, and a cut-heat temperature of 220°C for the test doses.

[16] The K-feldspar IRSL measurements were made on an automated Risø TL-DA-12 reader equipped with IR diodes for stimulation [Markey et al., 1997]. Aliquots containing several hundreds grains were prepared by mounting the grains in a monolayer on a 9.8 mm diameter aluminum disc with "Silkospay" silicone oil; this resulted in there being a greater number of grains of 63–80 μm diameter than grains of 212–250 μm in an aliquot. The
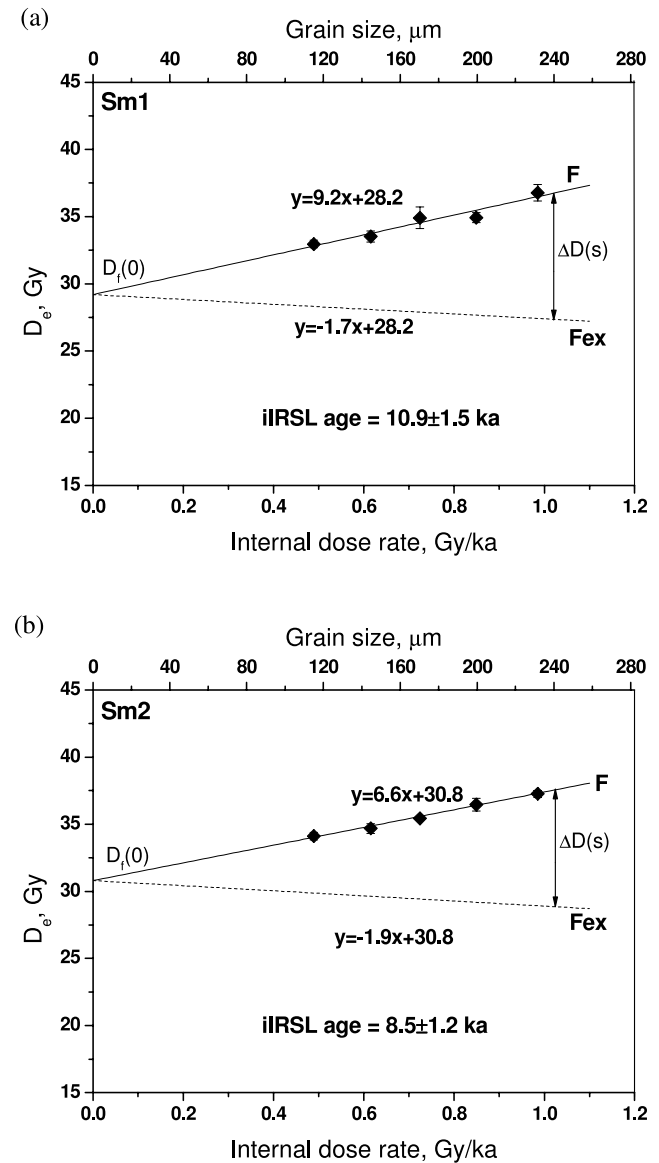

Figure 4. Isochron IRSL dating of samples Sm1, Sm2, Sm3, Sm4, and Sm5. The experimental data for K-feldspars (solid diamonds) were fitted by a linear function using the least squares method. Note the expanded y axis. The slope of Fex is dependent on the value of $D_f(0)$. For example, for samples (a) Sm1 and (b) Sm2 for which $D_f(0)$ is about 30 Gy, the slope of Fex is about −2. For samples (c) Sm3 and (d) Sm4 for which $D_f(0)$ is about 120 Gy, the slope of Fex is about −7. For sample (e) Sm5 for which $D_f(0)$ is about 200 Gy, the slope of Fex is about −12.

(c)

y=34x+119

F

ΔD(s)

$D_f(0)$

y=-7x+119

Fex

iIRSL age = 41 ± 6 ka

(d)

y=33x+116

F

ΔD(s)

$D_f(0)$

y=-7x+116

Fex

iIRSL age = 40 ± 6 ka

(e)

y=109x+200

F

ΔD(s)

$D_f(0)$

y=-12x+200
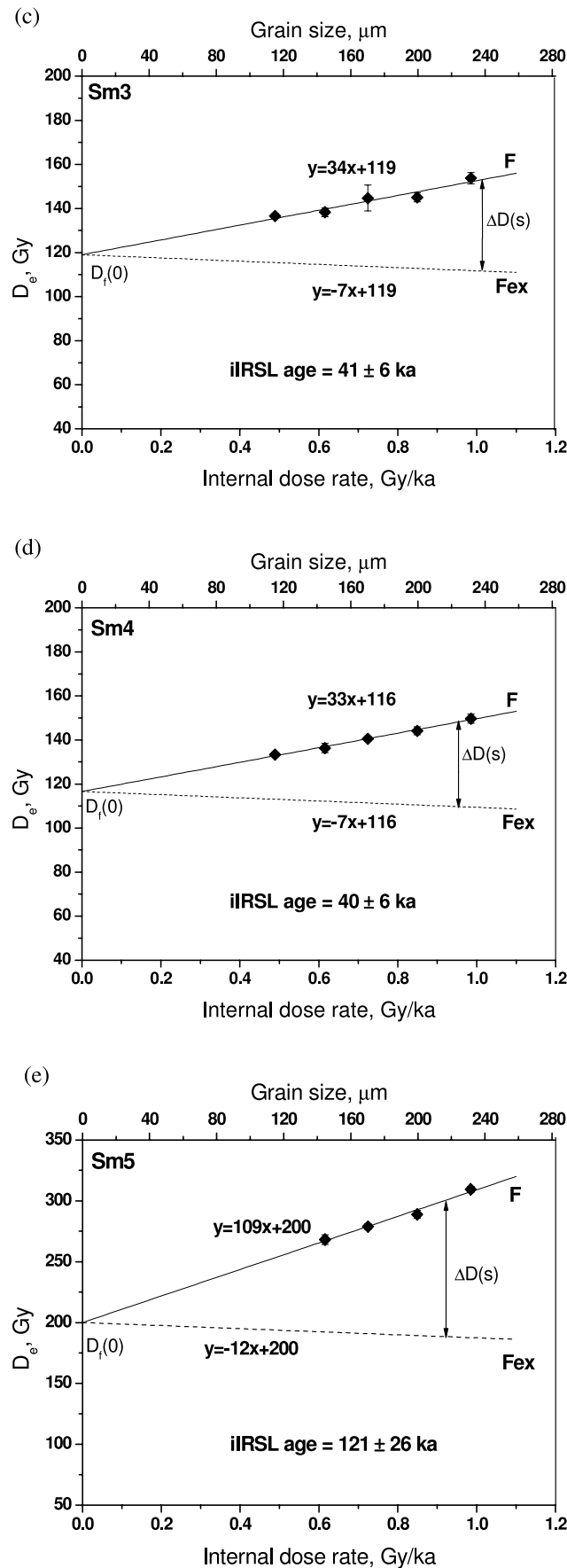
Fex

iIRSL age = 121 ± 26 ka

Figure 4.　(continued)

IRSL signals were detected using a photomultiplier tube with the IRSL passing through a filter pack containing Schott BG-39 and Corning 7−59 filters. The IRSL decay curve was measured at 60°C for 400 s. A SAR procedure was used [*Auclair et al.*, 2003] with the same preheat (10 s at 280°C) being applied to the natural, regenerative and test doses before their IR stimulation, as recommended by *Blair et al.* [2005]. The suitability of this procedure has been tested by application of a dose recovery experiment and a preheat plateau test [*B. Li et al.*, 2007]. All the IRSL measurement for regeneration doses (L_x) and test doses (T_x) were performed immediately after irradiation. Since the D_e values were determined using L_x/T_x, any fading-induced loss of signal after irradiation in L_x was corrected by T_x because they had a similar delay time after irradiation. At least six measurements were made for each grain size fraction and, as in the previous study of feldspar grains from sample HLD3 [*B. Li et al.*, 2007], a relative standard deviation (RSD) of ∼3% was obtained for each D_e value. Irradiations were carried out within the Risø reader using a ^{90}Sr/^{90}Y beta source, using a separate calibration of the dose rate for each grain size [*B. Li et al.*, 2007].

4. A New Isochron Dating Method (Isochron IRSL) Based on the Internal Dose in K-Feldspars

[17] In this paper we propose a new dating method, the physical basis of which is explained by *B. Li et al.* [2007]. The method is different from the earlier isochron procedure proposed by *Zhao and Li* [2002], which required measurement of D_e values of quartz grains for each grain size fraction. The new method is also different from the earlier isochron method alluded to by *B. Li et al.* [2007] which required measurement of D_e for quartz grains at one grain size. The new method requires measurements of D_e to be made only on K-feldspar grains. To distinguish it from these other isochron methods, we have termed it the isochron IRSL (isochron IRSL) method.

[18] Here we illustrate the isochron IRSL method using measured output for five samples, Sm1, Sm2, Sm3, Sm4, and Sm5. Figures 4a–4e shows the D_e values measured using the IRSL signals from K-feldspars as a function of the calculated internal dose rate (lower axis) relevant to the mean of the grain size range (upper axis). The high precision of each D_e value is seen by the error bar representing the standard error for at least six measurements being mostly smaller than the size of the symbol. A trend line F is obtained by fitting the D_e data with a linear function using the least squares method. As justified by *B. Li et al.* [2007], the function of F can be described as

$$D_f(s) = f\left(\dot{D}_{in} + \dot{D}_{ex}\right)t$$
$$= ft\left(1 - \frac{\dot{D}_{K\beta} + A_1\dot{D}_{U\beta} + A_2\dot{D}_{Th\beta}}{k}\right)\dot{D}_{in} + C_f, \qquad (1)$$

where f is the underestimation factor of the equivalent dose of K-feldspar (the ratio of measured value and true value), $C_f \approx f[\dot{D}_{K\beta} + \dot{D}_{U\beta} + \dot{D}_{Th\beta} + \dot{D}_{\gamma}]\,t = D_f(0)$, $\dot{D}_{U\beta}$, $\dot{D}_{Th\beta}$, $\dot{D}_{K\beta}$, and $\dot{D}_{\gamma}$ are the external beta dose rates from U, Th, and K and the gamma dose rate, respectively, and k, A_1, and A_2 are constants (see *B. Li et al.* [2007] for a full derivation).

[19] However, as suggested by *B. Li et al.* [2007], the IRSL related to the internal dose and external dose might have faded differently. Hence, it is necessary to reformulate the expression (equation 1) for the trend line *F*. Defining the underestimation factors for the internal doses and external doses as f_{in} and f_{ex}, respectively, the expression for *F* becomes

$$D_f(s) = f_{in}\dot{D}_{in}t + f_{ex}\dot{D}_{ex}t$$
$$= \left(f_{in}t - f_{ex}\frac{\dot{D}_{K\beta} + A_1\dot{D}_{U\beta} + A_2\dot{D}_{Th\beta}}{k}t\right)\dot{D}_{in} + C_f. \quad (2)$$

[20] Projection of the line *F* on to the *y* axis results in the value $D_f(0)$; this value represents the D_e that would be measured for infinitely small K-feldspar grains. This dose is derived entirely from external irradiation of the grains. Using this value of $D_f(0)$, it is possible to calculate the contribution of the external dose to the different grain sizes. This is achieved by multiplying this value (for the infinitely small grains) by the appropriate attenuation factors ($1 - \Phi(s)$) [*Mejdahl*, 1979], where $\Phi(s)$ is weighted according to the beta contributions from U, Th, K, and Rb in the bulk sediment. This is shown in Figures 4a–4e as the dashed line Fex. Mathematically, the function of Fex can be written as

$$D_{Fex}(s) = f_{ex}\dot{D}_{ex}(s)t = f_{ex}\frac{\dot{D}_{K\beta} + A_1\dot{D}_{U\beta} + A_2\dot{D}_{Th\beta}}{k}t\dot{D}_{in} + C_f. \quad (3)$$

Therefore, the difference between the line *F* and the dashed line Fex, $\Delta D(s) = f_{in}\dot{D}_{in}t$ (Figures 4a–4e), represents the internal dose received by grains of different sizes since they were last transported. Thus if $\Delta D(s)$ were to be plotted as a function of the internal dose rate, the slope would be $f_{in}t$. Since it has been suggested that the internal dose gives a reliable age [*B. Li et al.*, 2007], the value of f_{in} is expected to be 1 ($f_{in} = 1$); this means that the slope of $\Delta D(s)$ plotted against internal dose rate is an estimate of the true age t. A worked example of how to obtain an isochron IRSL age is provided in Appendix A using the data for SY3.

[21] Since no external dose rate appears after obtaining the difference between the two lines (*F* and Fex), there is no need to know the external dose rate using this isochron method. It is, therefore, particularly useful for sediments that have not experienced a constant dose rate through time, e.g., where water has resulted in the addition or removal of soluble radioactive isotopes. The value of $f_{in}t$ for each of these samples is given in Figures 4a–4e as the age. The error term on the age includes the uncertainty related to the intercept value obtained by extrapolation of the measured data set on to the *y* axis, the uncertainty associated with the scatter about the line of best fit to the limited number of data points (four or five), and the assumed uncertainty in the potassium content (see below).

5. Results
5.1. Internal Beta Dose Rate of K-Feldspar

[22] The internal beta dose rate (D_{in}) of K-feldspar is derived from radionuclides, mainly ^{40}K and ^{87}Rb, within the crystal lattice. The internal dose rate calculated for each

grain size fraction takes account of the noninfinite size (*s*) of the grains, such that $D_{in}(s) = D_{\infty}\Phi_K(s)$ where D_{∞} is the infinite beta dose rate due to ^{40}K and ^{87}Rb derived from the concentrations of K and Rb in the K-feldspar grains, and $\Phi_K(s)$ is the combined (^{40}K and ^{87}Rb) effective absorbed beta dose fraction for a grain of diameter *s* [*Aitken*, 1985, Appendix C]. Since the internal dose rate is largely dictated by the concentration of K within the K-feldspar grains extracted from the sediment samples, it is important to use the most appropriate K content for these grains. Values of $12.5 \pm 0.5\%$ and 400 ± 100 μg/g have been suggested for the K and Rb concentrations for separated K-feldspar fractions based on electron microprobe analyses of single grains [*Huntley and Baril*, 1997; *Huntley and Hancock*, 2001]. Similar values, 13.55 ± 0.09 % and 600 μg/g, were obtained by *Zhao and Li* [2005] for K and Rb contents measured by microprobe analyses of single grains.

[23] To test whether our separated K-feldspar grains have K and Rb contents similar to these values, different grain sizes fractions from three samples, Sm1, SY3, and HLD3, were measured using the Risø GM-25-5 beta counting technique [*Bøtter-Jensen and Mejdahl*, 1988]. This technique measures the total beta emission from the grains, and is unable to distinguish between beta particles from ^{40}K and ^{87}Rb and radionuclides in the uranium and thorium decay chains. However, using standards (containing both ^{40}K and ^{87}Rb), an equivalent K content (% K) can be obtained. The results are shown in Table 2. The K contents obtained for our samples mostly lie within the range of 10–14%, consistent with the values suggested in previous reports [*Huntley and Baril*, 1997; *Huntley and Hancock*, 2001; *Zhao and Li*, 2005]. For each sample, the K contents for different grain sizes are generally consistent with each other (i.e., within experimental errors). Smaller values were obtained for the smallest grain size (90–125 μm), presumably due to the fact that smaller grain sizes are more difficult to separate using heavy liquids and, therefore, contain more non-K-feldspar grains (e.g., Na-feldspar and quartz). However, such a small amount of contamination would have a negligible effect on the D_e measurement due to the high-IRSL sensitivity of K-feldspar when compared with Na-feldspar with the detection window (limited to violet/blue region by the BG-39 and Corning 7–9 color glass filters) used [*Huntley and Baril*, 1997]. This was confirmed by single grain IRSL measurements on K-feldspar fractions (Li, University of Hong Kong, unpublished Ph.D. thesis, 2007); in this study, it was found that almost all the grains giving detectable IRSL signals were K-feldspar. Therefore, it is reasonable to assume the same K content for all grain sizes. In the current study, the internal dose rate for each grain size fraction of K-feldspar was calculated using a K concentration of $13 \pm 1\%$ and a Rb concentration of 400 ± 100 μg/g. For each grain size, the dose rate from ^{87}Rb was calculated using the data of *Readhead* [2002] and that from ^{40}K was calculated using published absorbed beta dose fractions for spherical grains [*Brennan*, 2003; *Fain et al.*, 1999; *Mejdahl*, 1979].

5.2. Comparison of Isochron IRSL Ages, K-Feldspar IRSL Ages, and Quartz OSL Ages

[24] The results of applying the isochron IRSL method to all the samples are given in Table 1 (isochron IRSL age),
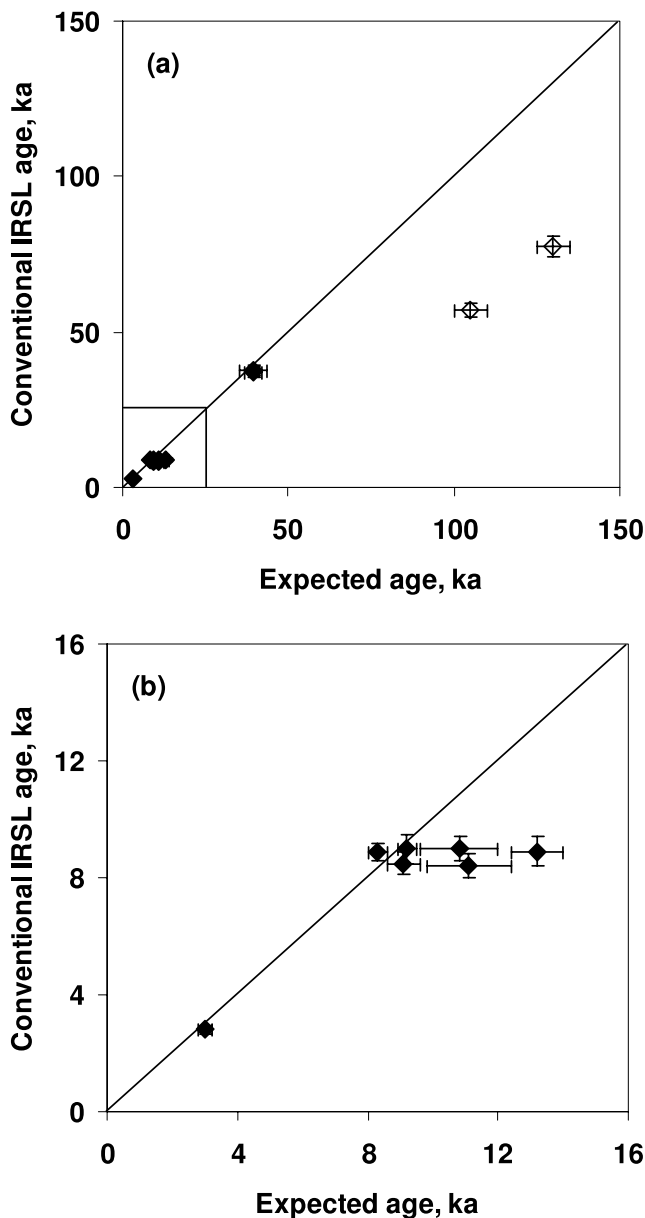
Figure 5. (a) Conventional K-feldspar IRSL ages plotted against the quartz OSL ages for 125–150 μm grains (solid diamonds) or the ages expected from independent chronological constraints (open diamonds). (b) The data shown in the square area in Figure 5a for samples younger than 15 ka.

together with the conventional IRSL ages for K-feldspars and quartz OSL ages, both obtained for grains of 125–150 μm diameter.

[25] In Figure 5, the ages based on conventional K-feldspar IRSL measurements for these samples are plotted as a function of the expected ages based on quartz for the same samples (Table 1). The comparison of quartz and K-feldspar IRSL ages is not shown for Dgw3 and Dgw4 because their environmental dose rates have changed significantly [*Li et al.*, 2008]. The IRSL ages are underestimated for half of the samples. The most severe age underestimation was found for the oldest samples Sm0404 and Sm5 (Figure 5a). Samples WG3, HLD3, and SY3 also show underestimation

in Figure 5b. For samples D4, Dgw5, Sm1, Sm2, Sm3, and Sm4, the IRSL ages are within error of the quartz OSL ages.

[26] The isochron IRSL ages obtained using the new method developed in this paper are compared with the quartz ages (or expected ages) in Figure 6; all data are plotted in Figure 6a and only data for samples younger than 15 ka in Figure 6b. The open symbols refer to samples Dgw3, Dgw4, Sm0404, and Sm5 that do not have a matching quartz age. There is good agreement between the isochron IRSL ages and the expected ages for all samples; they are consistent within 1σ. This agreement supports the assertion that use of the internal dose rate with the isochron data set results in the correct age being
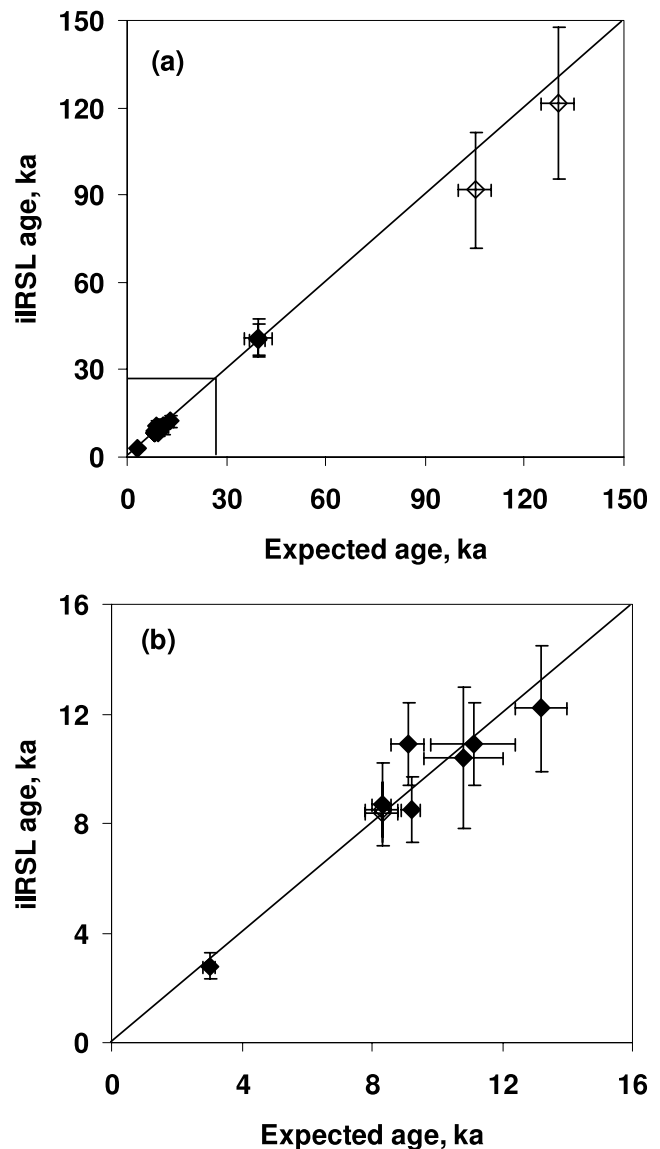

Figure 6. (a) The isochron IRSL ages, calculated using 13% K and 400 μg/g Rb, plotted against the quartz OSL ages (solid diamonds) or the expected ages (open diamonds). (b) The data shown in the square area in Figure 6a for samples younger than 15 ka. Solid diamonds represents comparison between isochron ages and quartz ages. The open symbols are for those samples that do not have a matching quartz age.
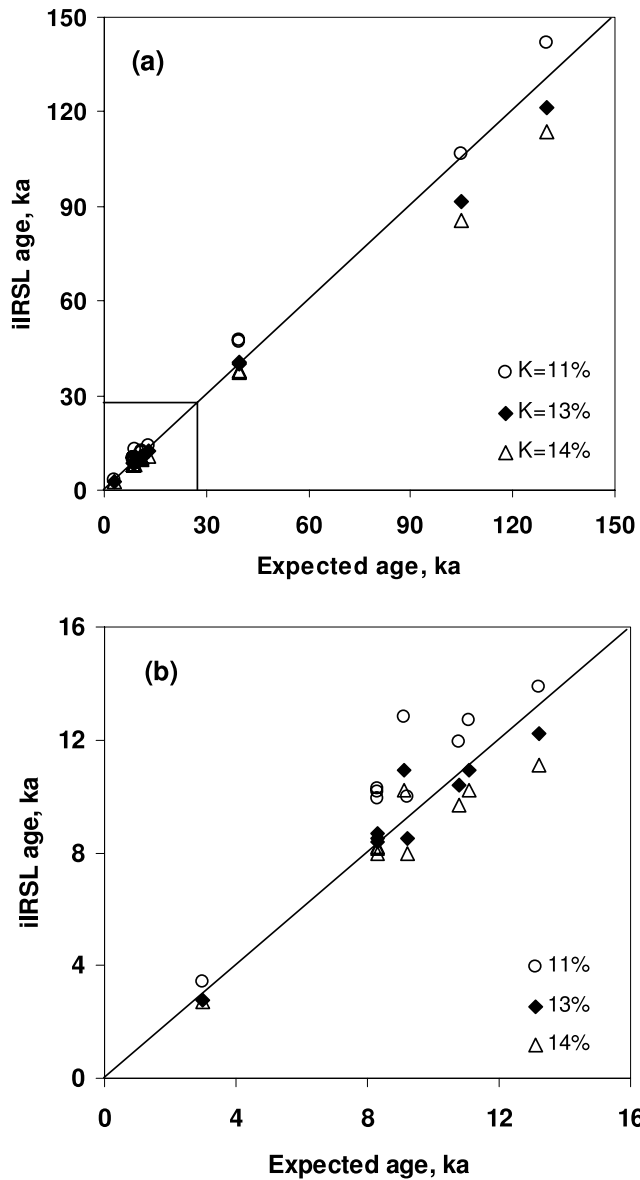
Figure 7. Isochron IRSL ages obtained by assuming different concentrations of potassium for K-feldspars (11, 13, and 14%), but keeping the Rb concentration as 400 μg/g, plotted against the expected ages. (b) The data shown in the square area in Figure 7a for samples younger than 15 ka.

obtained. This confirms the conclusion of *B. Li et al.* [2007] that the IRSL signal related to the internal dose rate does not fade (i.e., f_{in} = 1). We speculate that the decay of internal radioactive isotopes (i.e., [40]K and [87]Rb) into new isotopes (i.e., [40]Ca and [87]Sr) during the natural decay process may be the cause of different fading rates between the IRSL signal created by the radiation emanating from inside the K-feldspar crystal and that from outside. The radioactive decay might have created new defects and caused changes in the crystal microstructure, which might either create stable (or nonfading) traps or prevent the tunneling process of the trapped electrons related to these defects. Unfortunately, at the present time, there is little we can do more than speculate. More fundamental studies on the mechanism are needed.

5.3. Sensitivity of Isochron IRSL Ages to K and Rb Values

[27] The isochron IRSL ages in Figure 6 were obtained using only the internal dose rate to the K-feldspar grains based on values of potassium and rubidium assumed to be most likely for such grains, i.e., values close to those measured by *Huntley and Baril* [1997] and by *Zhao and*
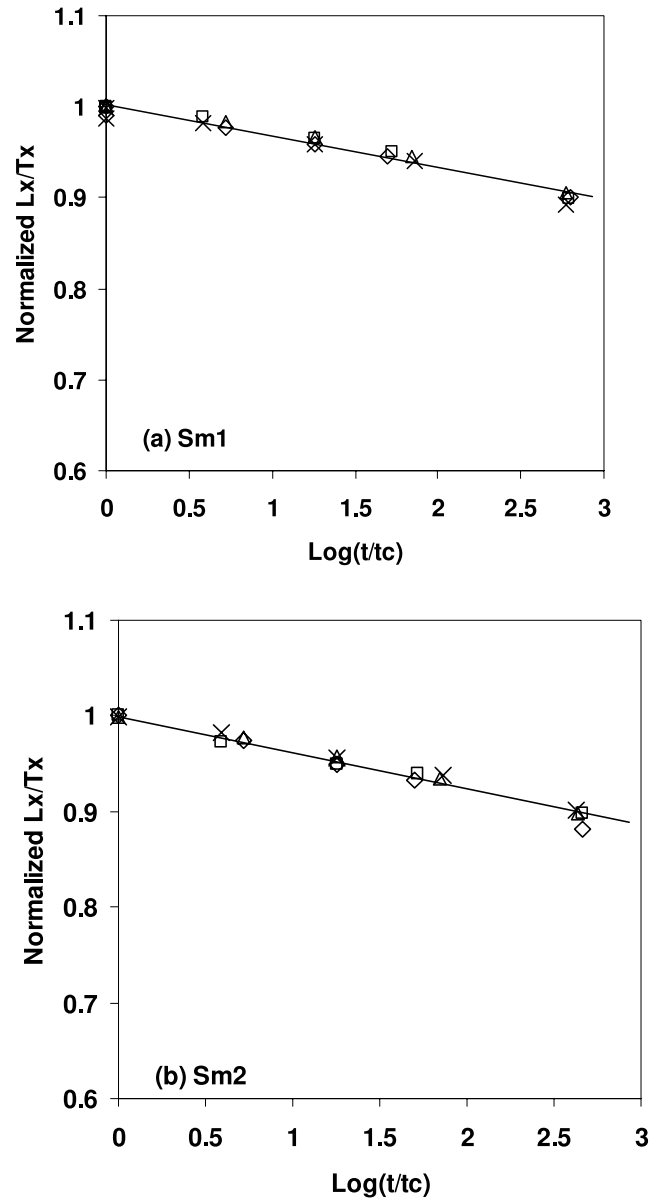

Figure 8. Anomalous fading data for samples (a) Sm1, (b) Sm2, (c) Sm3, and (d) Sm4. Each symbol (square, triangle, diamond, and cross) represents one of the four aliquots investigated for each sample. Each sample was bleached by IR and then given a dose of ~34 Gy prior to fading measurements. L_x/T_x is the sensitivity-normalized IRSL and is shown as a function of $\log(t/t_c)$, where t is the storage time (defined as the time elapsed since the midpoint of irradiation [*Aitken*, 1985]) and t_c is the time for the prompt measurement [*Huntley and Lamothe*, 2001]. Data are normalized to the value for the prompt measurement (i.e., for log t/t_c = 0).
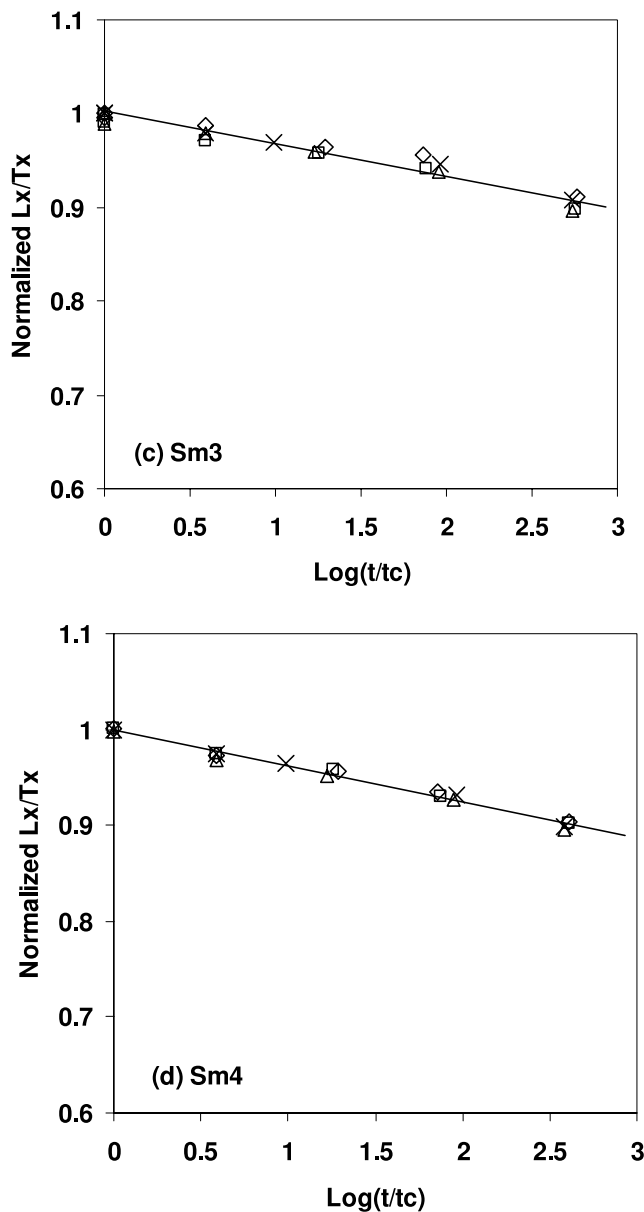
Figure 8.   (continued)

Li [2005] and the rubidium concentration recommended by *Huntley and Hancock* [2001]. The isochron IRSL method is sensitive to the choice of potassium content, but the value of 13% generally produces ages in closer agreement with independent constraints than is the case for K contents of 11–14% (with the concentration of Rb maintained at 400 μg/g) (Figure 7). Our uncertainty in the exact value to use is reflected in the error term associated with the age, which is dominated by the ±1% attached to the K content of 13%.

5.4. Fading-Corrected Conventional IRSL Ages

[28] Laboratory fading tests (*g* value measurements [*Aitken*, 1985]) for nine samples were carried out using the method proposed by *Auclair et al.* [2003]. It should be noted that in this measurement, the samples were exposed to laboratory irradiation after optical bleaching (i.e., solely an external source of dose), whereas the natural samples were exposed to both internal and external sources of ionizing

radiation. Four K-feldspar aliquots from each sample were measured using the 125–150 μm grain size; similar measurements had been carried out previously for samples WG3, HLD3, and SY3 [*B. Li et al.*, 2007]. Figure 8 shows the fading results of samples Sm1, Sm2, Sm3, and Sm4. Good linearity with (log) time was obtained and there is little variation among different aliquots of the same sample [cf. *Huntley and Lian*, 2006]. A typical value of ~3% per decade (the first measurement time t_c = 430 s) was obtained for all samples measured (Table 1). We presume that these samples have similar fading rates within errors, partly because most the samples are from the same geographical area and the minerals contained in them are, therefore, likely to originate from the same source.

[29] These measured *g* values were used to correct the conventional IRSL ages for the 125–150 μm grains using the method proposed by *Huntley and Lamothe* [2001]. The corrected IRSL ages are shown in Table 1 (last column) and are compared with the quartz OSL ages (or expected ages) in Figure 9. For young samples with ages of less than 50 ka, only HLD3, WG3 and SY3 showed agreement with the independent age control. For the other samples (Dgw5, Sm1, Sm2, Sm3, and Sm4) application of the fading correction resulted in the corrected IRSL ages exceeding their expected ages by ~35%; this cannot be compensated for by including an additional internal dose rate contributed from alpha particles (~10% of the total dose rate). For the oldest pair of samples Sm0404 and Sm5, their D_e values are beyond the linear dose response range, and hence, application of the fading correction method proposed by *Huntley and Lamothe* [2001] was inappropriate [*Huntley and Lian*, 2006]. If the correction were applied, it would be expected to result in age underestimation and, as anticipated, the corrected IRSL ages are 26% and 24% younger than the expected ages for Sm0404 and Sm5, respectively (Table 1).

6. Discussion

[30] From the comparisons given in Figures 5, 6, and 9, the closest agreement between the quartz OSL age (or independent age) and measurements made with K-feldspars was obtained using the isochron IRSL method. This confirms the conclusion reached by *B. Li et al.* [2007] that the IRSL signal related to the internal dose gives reliable ages. This can be investigated further by looking at the correlation between the extent of age underestimation and the external dose rate (Table 1). A negative correlation can be observed between the ratio of K-feldspar IRSL age (conventional and not corrected for fading) and the quartz OSL age and the external dose rate (Figure 10) for samples with an age of ~10 ka, i.e., Sm1, Sm2, Dgw5, SY3, HLD3, and WG3 (solid diamonds). On the basis of Figure 10, we recognized two distinct data sets that show this behavior: the upper set of samples (Sm1, Sm2, and Dgw5) and the lower set of samples (HLD3, SY3, and WG3). This suggests that the K-feldspar grains that received a higher proportion of the total dose rate from external sources give greater underestimations of the IRSL age. Samples with different ages are also shown for comparison, i.e., D4 (open diamond) Sm3, Sm4, Sm0404 and Sm5 (open triangles). Since there might be a dependence of fading rate (and, hence, age underestimation) on dose [*Huntley and Lian*, 2006; *Wallinga et al.*,
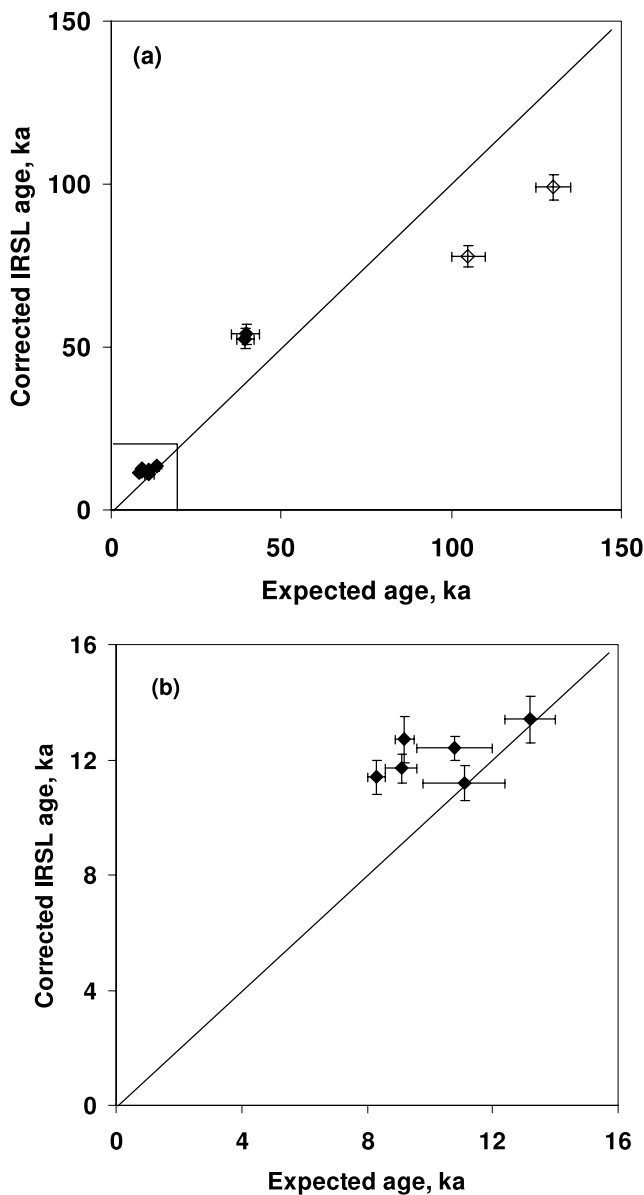
Figure 9. (a) The corrected IRSL ages obtained using the measured g values (Table 1), plotted against the quartz OSL ages (solid diamonds) or expected ages (open diamonds). (b) The data shown in the square area in Figure 9a for samples younger than 15 ka.

2007], any comparison between samples that span a wide age range could complicate the interpretation of the relationship between age underestimation and external dose rate. To address this problem, further studies on the dose dependence of fading rate and its effect on age underestimation are needed. If only the dose derived from outside the grain had faded, extrapolation of the data set in Figure 10 onto the y axis should give an age ratio of 1, corresponding to an external dose rate of 0 Gy/ka. However, the data set in Figure 10 gives a ratio of 1 for an external dose rate of ∼2– 2.5 Gy/ka. One possible reason for this discrepancy is that only a limited number of samples of the same age are compared. Another possible reason is that the IRSL age might be overestimated for those samples having a consid-

erable U and Th content within the K-feldspar grains. For the K-feldspar grains of sample D4, *Zhao and Li* [2005] obtained values of 0.60 ± 0.02 μg/g and 2.92 ± 0.09 μg/g for the U and Th contents, respectively; these amount to an effective internal alpha dose rate of 0.33 ± 0.01 Gy/ka for grains larger than 100 μm in diameter. If this contribution is included in the total dose rate, then the IRSL age would be reduced by 7%. If a similar value for the internal alpha dose rate is used for other samples, the IRSL ages shown in Table 1 are reduced by ∼10%, thereby making them younger than the quartz OSL ages. This could contribute significantly to the internal alpha dose rate and thus the internal dose rate might have been underestimated. However, as will be shown later, isochron IRSL ages are insensitive to the internal U and Th concentrations.

[31] The possible underestimation of the internal alpha dose rate produced by U and Th contents within K-feldspar grains may also explain the similarity of the conventional IRSL ages and the quartz ages for samples D4, Dgw5, Sm1, Sm2, Sm3, and Sm4, a result that seems to contradict the laboratory fading test (Table 1). The observation that these samples show detectable loss of signal in fading tests suggests these samples should have suffered from some anomalous fading since deposition. We must, therefore, consider the possibility that the conventional IRSL ages might have been overestimated. Since the robustness of the D_e measurement protocol for K-feldspars has been demonstrated [*B. Li et al.*, 2007], there is no reason to doubt the validity of D_e estimation. However, an overestimation of the IRSL age could have been caused by an underestimation of the dose rate, due perhaps to presence of significant quantities of U and Th within the K-feldspar grains that were unaccounted for. In this case, the internal U and Th would
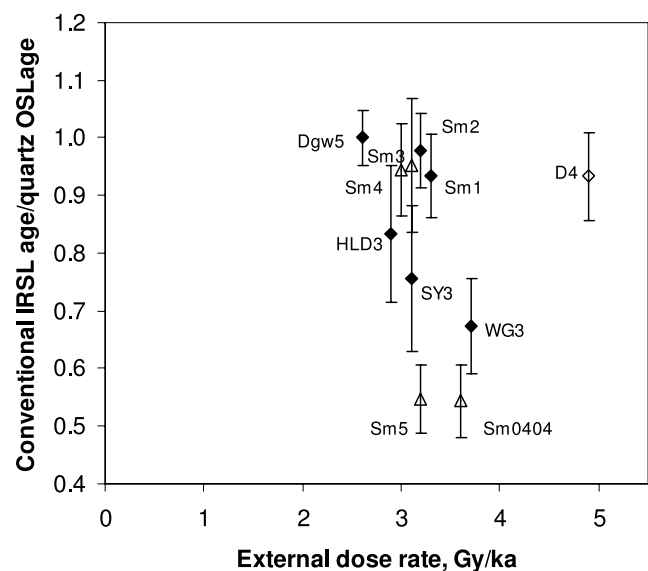

Figure 10. Ratios of conventional IRSL age to quartz OSL age for 125–150 μm diameter grains, plotted against the external dose rates. Solid diamonds represent samples with an age of ∼10 ka, i.e., Sm1, Sm2, Dgw5, SY3, HLD3, and WG3. Open symbols are the samples with different ages, i.e., D4 (open diamond) and Sm3, Sm4, Sm0404, and Sm5 (open triangles).

contribute equally to the dose rate for all grain sizes, and thus cause the isochron (F) to slide in parallel or vertically along the y axis (D_e) in the isochron plot. Therefore, this extra internal dose rate would have a negligible effect on the slope of the isochron, and thus on the isochron IRSL age.

[32] The results from the new isochron IRSL procedure have been obtained without the necessity of obtaining information from the measurements of quartz, as was required in the previous isochron procedures [*B. Li et al.*, 2007; *Zhao and Li*, 2002]. This reduces sample preparation and measurement time, and enables dating of samples for which D_e values cannot be obtained for quartz because of saturation of the fast OSL component; i.e., it can be applied to older samples (>70 ka). The new isochron IRSL method also reduces the size of the age uncertainties by avoiding having to propagate the errors associated with the extra set of measurements on quartz; in addition, D_e values from quartz are usually more scattered [*S.-H. Li et al.*, 2007a]. An important prerequisite of applying the isochron IRSL method is that the K-feldspar grains must be well bleached and are not a mixture of grains of different ages; thus a homogeneous D_e distribution can be obtained for each grain size fraction, and the potentially different bleaching histories of grains of different size are not an issue. For partially bleached or postdepositionally mixed samples, e.g., fluvial sediments, use of large aliquots, as described in the paper, would result in incorrect ages. However, this method may still have potential for dating these samples by plotting the "minimum age model" (MAM) [*Galbraith et al.*, 1999] D_e values obtained from measurements made on single K-feldspar grains as a function of their internal dose rate. This would work provided that the MAM values are sufficiently accurate and the extent of bleaching experienced by grains of different sizes at the time of deposition is not affected during the process of grain transport in streams.

[33] The data presented in Table 1 and Figure 5 indicate different degrees of underestimation in the conventional IRSL ages compared to the quartz ages or expected ages. This suggests that the K-feldspars from the different samples used in this study have experienced different fading rates since deposition. However, a similar g value of ∼3% was found in the laboratory fading measurements for all the samples investigated (Table 1). When the IRSL ages were corrected for fading using the laboratory-measured fading rates [*Huntley and Lamothe*, 2001], we obtained age overestimates for some of the young samples (<50 ka) and, therefore, deduce that the laboratory fading rate is not necessarily equivalent to the fading rate experienced in nature. *Wallinga et al.* [2007] found that the measured fading rate (2.6% per decade) for the separated K-feldspar grains in their study was too small to bring the corrected IRSL ages into alignment with the quartz OSL ages. They also observed that applying a fading rate of 5% per decade resulted in overcorrection of the ages for the younger samples and undercorrection for the older samples. This led them to propose that fading is dependent on D_e and dose rate. A similar conclusion had already been reached by *Huntley and Lian* [2006] who observed an increase of fading rate with absorbed dose from 3.1%/decade at 175 Gy to 6.0%/decade at ∼350 Gy for a bleached sample. For naturally saturated sample, 13%/decay was observed.

[34] An important implication of our study (e.g., Figures 8 and 10) is that two populations of trapped charge give rise to the IRSL signal: one of these populations is unstable (fading), while the other is stable (nonfading). During natural irradiation, the stable charges are related to both the internal dose and external dose, whereas the unstable charges are only related to the external dose. During laboratory irradiation, both kinds of IRSL signal are generated at the same time since the irradiation source is external to the grains. It is thus expected that the production rates of the two populations of charges may be different for the natural irradiation and the laboratory irradiation, owing to the competition related to the internal dose rate during natural irradiation. For young samples (e.g., <50 ka) with low doses, depending on the proportion of fading and nonfading traps and the ratio of internal to external dose rates, the effective fading rate of the natural sample might be lower than that measured in the laboratory because of the preferential filling of nonfading traps by the internal dose rate. This would partly explain why the conventional IRSL ages corrected for fading are overestimated for some young samples in our study. On the other hand, for older samples, the effective natural fading rate may be higher than the laboratory fading rate because the fading traps might have experienced repeated filling and emptying, and because of the dependences of the fading rate on D_e and dose rate [*Huntley and Lian*, 2006; *Wallinga et al.*, 2007]. Unfortunately, as stated by *Huntley and Lamothe* [2001], their correction method should not be applied to "old" samples, e.g., Sm0404 and Sm5. Because there is currently no appropriate correction method that can be applied to older samples to support this assertion, the exact reason for the shortfall in the fading-corrected ages of samples Sm0404 and Sm5 remains unresolved. However, the success of the fading correction for some samples in this study and many other samples in a number of studies [*Auclair et al.*, 2007; *Buylaert et al.*, 2007; *Lamothe*, 2004; *Van Heteren et al.*, 2000; *Wolfe et al.*, 2006] appears to indicate that there may be a balance of these effects that enables the fading correction to work, at least for samples in the low-dose (linear) region of the dose response.

7. Conclusions

[35] A new isochron IRSL dating method (isochron IRSL) is proposed for K-feldspars extracted from well-bleached sediments. The age calculation is based on the measurement of the equivalent dose for grains of different size. The IRSL method exploits the constant dose rate contribution from potassium (and associated rubidium) within such grains. It also capitalizes on the high precision that can be achieved for D_e measurements using K-feldspars, and, since the dose response of the IRSL signal of K-feldspar grains reaches higher doses than the fast component OSL signal of quartz, older ages can be obtained. The isochron IRSL measurement procedure appears to overcome problems associated with anomalous fading, including what to do with samples for which the natural IRSL signal of the K-feldspars is beyond the linear region of the dose response curve. It also avoids the effect of changes in the past environmental dose rate, as the age is determined using only the internal dose rate and measured D_e values. The method is also immune to the

Table A1. Summary of the Data Used for Constructing the Isochron Plot for Sample SY3

Grain Size (μm)	$D_f(s)$ (Gy)	$\Phi_K(s)^a$	Absorbed Dose From $^{87}Rb^b$ (mGy/μg/g)	$\dot{D}_{in}(s)$ (Gy/ka)	$D_{Fex}(s)$ (Gy)	External Dose Rate^c (Gy/ka)
90–125	29.4 ± 0.3 (n = 8)	0.0412	0.175	0.49 ± 0.04	23.7	2.82
125–150	30.3 ± 0.5 (n = 7)	0.0523	0.209	0.62 ± 0.05	23.5	2.80
150–180	31.3 ± 0.3 (n = 7)	0.0624	0.225	0.72 ± 0.05	23.3	2.78
180–212	32.6 ± 0.3 (n = 8)	0.0738	0.247	0.85 ± 0.06	23.1	2.76
212–250	33.9 ± 0.4 (n = 6)	0.0867	0.259	0.99 ± 0.07	22.9	2.73

^{a}The values of beta absorption coefficient as a function of grain size for the decay of ^{40}K, $\Phi_K(s)$, are taken from *Fain et al.* [1999] by interpolation of the values they provided.

^{b}The values of the absorbed dose from ^{87}Rb are taken from *Readhead* [2002] by interpolation of the values provided by him.

^{c}The external dose rates were calculated using the typical values of environmental U, Th, and K contents; water content; and cosmic ray (K = 1.5%, U = 3 μg/g, Th = 10 μg/g, no radon loss, water content = 10%, and cosmic ray dose rate = 0.2 Gy/ka). These values give rise to a combined beta, gamma, and cosmic dose rate of 2.93 Gy/ka for infinitely small grains.

complications attendant on water content variations as the water content only affects the external dose rate. While the isochron IRSL method has been developed using sediments from the boundary between the loess and sand area in China, it should be applicable worldwide to any (well-bleached) deposits that contain a mix of fine, medium and coarse sand-sized grains of K-feldspar. Further testing of the isochron IRSL method is required using samples with better independent age control.

Appendix A

[36] The step-by-step procedure of constructing the isochron plot and calculating the isochron IRSL age is listed below, using data for sample SY3.

A1. D_e Measurements

[37] The D_e values ($D_f(s)$) from K-feldspar of different grain sizes (90–125, 125–150, 150–180, 180–212, and 212–250 μm in diameter) were measured (column 2 in Table A1 with the number of aliquots n measured for each grain size) using the modified SAR protocol (section 3 of main text). A typical dose response curve of the IRSL signal from a single aliquot of 90–125 μm grains of K-feldspar of sample SY3 and the D_e distribution histogram of the 90–125 μm grains are shown in Figures A1a and A1b, respectively.

A2. Calculating Internal Dose Rate for Different Grain Sizes

[38] Assuming a K-content of 13% and a Rb-content of 400 μg/g, the internal beta dose rate $\dot{D}_{in}(s)$ can be calculated using the following equation

$$\dot{D}_{in}(s) = D_K\Phi_K(s) + D_{Rb}\Phi_{Rb}(s), \qquad (A1)$$

where $\Phi_K(s)$ and $\Phi_{Rb}(s)$ are the appropriate beta absorption coefficients for K and Rb, as given by *Fain et al.* [1999] and *Readhead* [2002]; $D_K = 0.782C_K = 10.17$ Gy/ka and $D_{Rb} = 0.019C_{Rb}/50 = 0.152$ Gy/ka are the infinite beta dose rate for specific concentrations of K ($C_K = 13\%$) and Rb ($C_{Rb} = 400$ μg/g) in the K-feldspar grains (conversion factors from *Adamiec and Aitken* [1998]). The values of $\Phi_K(s)$ [*Fain et al.*, 1999] and absorbed dose per μg/g Rb ($D_{Rb}\Phi_{Rb}(s)/C_{Rb}$) [*Readhead*, 2002] are listed in Table A1, and the calculated values of $\dot{D}_{in}(s)$ are also listed.
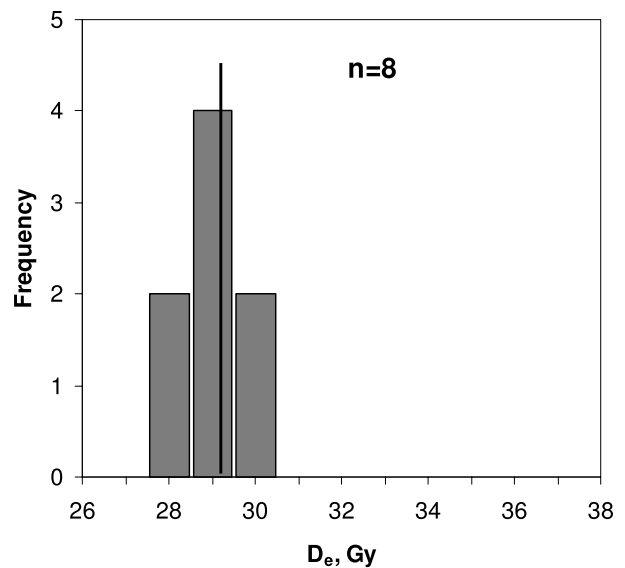
(a)
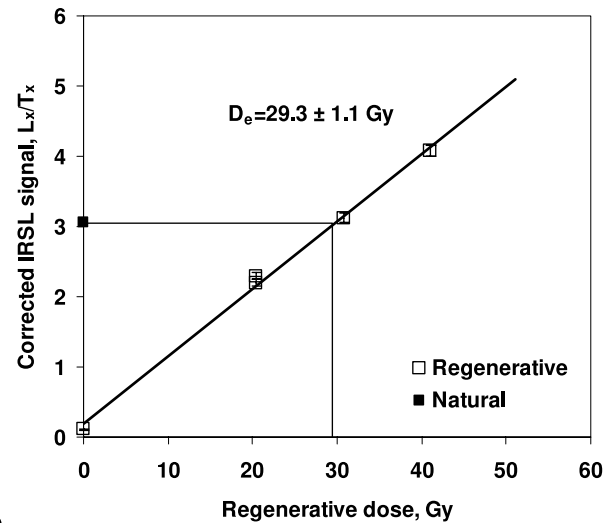
(b)

Figure A1. (a) The dose response curve of the IRSL signal from a single aliquot of 90–125 μm grains of K-feldspar from SY3. (b) Histogram of K-feldspar IRSL D_e values from 90 to 125 μm grains from sample SY3. The vertical line represents the D_e value for the aliquot shown in Figure A1a.
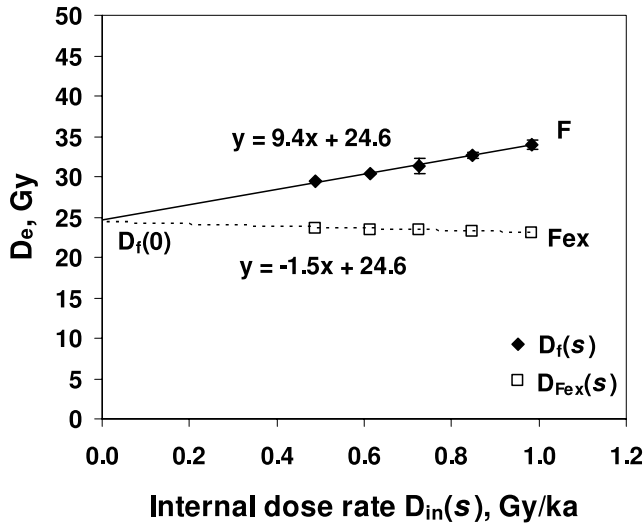
Figure A2. The isochron plot of sample SY3. The measured $D_e(s)$ values (solid diamonds) and the calculated $D_{Fex}(s)$ values (open squares) for K-feldspars were fitted by linear functions (shown on the figure) using the least squares method.

A3. Constructing Isochron F

[39] The measured values of $D_f(s)$ from Table A1 are plotted against the corresponding internal dose rates $\dot{D}_{in}(s)$ in Figure A2. The data points of $D_f(s)$ (solid diamonds) are then fitted using a linear regression. A trend line (F) is obtained, and its function is $y = 9.4x + 24.6$. The intercept $D_f(0) = 24.6$ Gy, represents the D_e for infinitely small grains. The slope, 9.4 ± 1.4, has the unit of ka.

A4. Constructing Isochron Fex

[40] Using the value of $D_f(0) = 24.6$ Gy, the external doses $(D_{fex}(s))$ for K-feldspar of a specified grain size (s) can be estimated from the following equation:

$$\frac{D_{Fex}(s)}{\dot{D}_{ex}(s)} = \frac{D_f(0)}{\dot{D}_{ex}(0)}, \tag{A2}$$

where $\dot{D}_{ex}$ (s) is the external dose rate for grain size s. The value of $\dot{D}_{ex}$ (s) can be estimated on the basis of the environmental K, U, and Th concentrations, cosmic ray flux and burial depth, and the attenuation factor $(1 - \Phi(s))$ for external beta irradiation [Fain et al., 1999]. The values of $\Phi(s)$ (the attenuation coefficient) differ slightly for the natural beta flux, depending upon the maximum beta energy of each emitter, e.g., ^{40}K or individual isotopes in the uranium and thorium decay chains.

[41] The slope of the line Fex in the isochron plot is thus given as

$$S_{Fex} = \frac{D_{Fex}(s) - D_f(0)}{\dot{D}_{in}(s)} = \frac{D_f(0)}{\dot{D}_{in}(s)} \left(\frac{\dot{D}_{ex}(s)}{\dot{D}_{ex}(0)} - 1 \right). \tag{A3}$$

However, as justified by Li et al. [2008], the value of $\dot{D}_{ex}$ (s) has negligible effect on the slope of Fex; thus one can simply assume typical values of environmental U, Th, and K contents, water content and cosmic ray (e.g K = 1.5%,

U = 3 μg/g, Th = 10 μg/g, no radon loss, water content = 10% and cosmic ray dose rate = 0.2 Gy/ka). The external dose rates calculated using these typical values are listed in Table A1.

[42] $D_f(0)$ was estimated as 24.6 ± 1.1 Gy by extrapolation (see section 3) and the calculated external dose rate of the infinitely small grains $\dot{D}_{ex}$ (0) = 2.93 Gy/ka. It is noted that $\dot{D}_{ex}$ (0) does not include the external alpha dose rate; the reason for this is that the estimated value of $D_f(0)$ also does not include the external alpha dose because it is obtained by extrapolation from measured values for the larger grain sizes whose outer layers were removed by HF etching. Using these values in equation (A2), and inserting the external dose rate for grains of 212–250 μm $\dot{D}_{ex}$ (212– 250) = 2.73 Gy/ka, yields the externally derived dose as $D_{Fex}(212-250) = (24.6/2.93)*2.73 = 22.9$ Gy. Values of $D_{Fex}(s)$ are calculated for all the grain sizes for which there are measurements of the equivalent dose. In this case, the values of $D_{Fex}(s)$ for grain sizes 90–125, 125–150, 150– 180, 180–212, and 212–250 μm in diameter are calculated and listed in Table A1. These values are shown in Figure A2 (open squares) and a linear fit of these points gave a function $y = -1.5x + 24.6$. The slope, -1.5 ± 0.1, has the unit of ka.

A5. Calculating Isochron IRSL Age

[43] The isochron IRSL age t is then obtained as the difference between the slopes of F (9.4 ± 1.4) and Fex (-1.5 ± 0.1) (see text for justification). Thus for SY3, the isochron IRSL age is t = 9.4 + 1.5 = 10.9 ± 1.5 ka. The error in the isochron IRSL age is calculated from the errors of the two slopes; these are given during linear regression of the two data sets (F and Fex). Thus, the isochron IRSL age is 10.9 ± 1.5 ka (as given in Table 1 of the main text).

References

Adamiec, G., and M. J. Aitken (1998), Dose-rate conversion factors: Update, *Ancient TL*, 16, 37–50.
Aitken, M. J. (1985), *Thermoluminescence Dating*, Academic, London.
Aitken, M. J. (1998), *An Introduction to Optical Dating*, Oxford Univ. Press, Oxford, U. K.
Auclair, M., M. Lamothe, and S. Huot (2003), Measurement of anomalous fading for feldspar IRSL using SAR, *Radiat. Meas.*, 37, 487–492, doi:10.1016/S1350-4487(03)00018-0.
Auclair, M., M. Lamothe, E. Lagroix, and S. K. Banerjee (2007), Luminescence investigation of loess and tephra from Halfway House section, Central Alaska, *Quat. Geochronol.*, 2, 34–38, doi:10.1016/j.quageo.2006.05.009.
Blair, M. W., E. G. Yukihara, and S. W. S. McKeever (2005), Experiences with single-aliquot OSL procedures using coarse-grain feldspars, *Radiat. Meas.*, 39, 361–374, doi:10.1016/j.radmeas.2004.05.008.
Bøtter-Jensen, L., and V. Mejdahl (1988), Assessment of beta-dose-rate using a GM multicounter system, *Nucl. Tracks Radiat. Meas.*, 14, 187–191, doi:10.1016/1359-0189(88)90062-3.
Bøtter-Jensen, L., S. W. S. McKeever, and A. G. Wintle (2003), *Optically Stimulated Luminescence Dosimetry*, Elsevier, Amsterdam.
Brennan, B. J. (2003), Beta doses to spherical grains, *Radiat. Meas.*, 37, 299–303, doi:10.1016/S1350-4487(03)00011-8.
Buylaert, J. P., D. Vandenberghe, A. S. Murray, S. Huot, and F. De Corte (2007), Luminescence dating of old (>70 ka) Chinese loess: A comparison of single-aliquot OSL and IRSL techniques, *Quat. Geochronol.*, 2, 9–14, doi:10.1016/j.quageo.2006.05.028.

Fain, J., S. Soumana, M. Montret, D. Miallier, T. Pilleyre, and S. Sanzelle (1999), Luminescence and ESR dating Beta-dose attenuation for various grain shapes calculated by a Monte-Carlo method, *Quat. Sci. Rev.*, *18*, 231–234, doi:10.1016/S0277-3791(98)00056-0.

Galbraith, R. F., R. G. Roberts, G. M. Laslett, H. Yoshida, and J. M. Olley (1999), Optical dating of single and multiple grains of quartz from Jinmium rock shelter, Northern Australia: Part I. Experimental design and statistical models, *Archaeometry*, *41*, 339–364, doi:10.1111/j.1475-4754.1999.tb00987.x.

Huntley, D. J., and M. R. Baril (1997), The K content of the K-feldspars being measured in optical dating or in thermoluminescence dating, *Ancient TL*, *15*, 11–13.

Huntley, D. J., and R. G. V. Hancock (2001), The Rb contents of the K-feldspars being measured in optical dating, *Ancient TL*, *19*, 43–46.

Huntley, D. J., and M. Lamothe (2001), Ubiquity of anomalous fading in K-feldspars and the measurement and correction for it in optical dating, *Can. J. Earth Sci.*, *38*, 1093–1106, doi:10.1139/cjes-38-7-1093.

Huntley, D. J., and O. B. Lian (2006), Some observations on tunneling of trapped electrons in feldspars and their implications for optical dating, *Quat. Sci. Rev.*, *25*, 2503–2512, doi:10.1016/j.quascirev.2005.05.011.

Imbrie, J., J. D. Hays, D. B. Martinson, A. McIntyre, A. C. Mix, J. J. Morley, N. G. Pisias, W. L. Prell, and N. J. Shackleton (1984), The orbital theory of Pleistocene climate: Support from a revised chronology of the marine δ^{18}O record, in *Milankovitch and Climate*, edited by A. I. Berger et al., pp. 269–305, D. Reidel, Dordrecht, Netherlands.

Lamothe, M. (2004), Optical dating of pottery, burnt stones, and sediments from selected Quebec archaeological sites, *Can. J. Earth Sci.*, *41*, 659–667, doi:10.1139/e04-032.

Lamothe, M., and M. Auclair (1999), A solution to anomalous fading and age shortfalls in optical dating of feldspar minerals, *Earth Planet. Sci. Lett.*, *171*, 319–323, doi:10.1016/S0012-821X(99)00186-8.

Lamothe, M., M. Auclair, C. Hamzaoui, and S. Huot (2003), Towards a prediction of long-term anomalous fading of feldspar IRSL, *Radiat. Meas.*, *37*, 493–498, doi:10.1016/S1350-4487(03)00016-7.

Li, B., S.-H. Li, A. G. Wintle, and H. Zhao (2007), Isochron measurements of naturally irradiated K-feldspar grains, *Radiat. Meas.*, *42*, 1315–1327, doi:10.1016/j.radmeas.2007.09.008.

Li, B., S.-H. Li, A. G. Wintle, and H. Zhao (2008), Overcoming environmental dose rate changes in luminescence dating of waterlain deposits, *Geochronometria*, doi:10.2478/v10003-008-0003-z, in press.

Li, S.-H., and J. M. Sun (2006), Optical dating of Holocene dune sands from the Hulun Buir Desert, northeastern China, *Holocene*, *16*, 457–462, doi:10.1191/0959683606hl942rr.

Li, S.-H., J. M. Sun, and H. Zhao (2002), Optical dating of dune sands in the northeastern deserts of China, *Palaeogeogr. Palaeoclimatol. Palaeoecol.*, *181*, 419–429, doi:10.1016/S0031-0182(01)00443-6.

Li, S.-H., Y. Y. Chen, B. Li, J. M. Sun, and L. R. Yang (2007), OSL dating of sediments from desert in northern China, *Quat. Geochronol.*, *2*, 23–28, doi:10.1016/j.quageo.2006.05.034.

Li, X. G., G. L. Liu, G. Y. Xu, F. C. Li, F. L. Wang, and K. S. Liu (1984), Dating the age of the Ordos man and Sjara Osso Gol culture, paper presented at 1st National [14]C Conference, Sci. Press, Beijing.

Markey, B. G., L. Bøtter-Jensen, and G. A. T. Duller (1997), A new flexible system for measuring thermally and optically stimulated luminescence, *Radiat. Meas.*, *27*, 83–89, doi:10.1016/S1350-4487(96)00126-6.

Mejdahl, V. (1979), Thermoluminescence dating: Beta-dose attenuation in quartz grains, *Archaeometry*, *21*, 61–72, doi:10.1111/j.1475-4754.1979.tb00241.x.

Murray, A. S., and A. G. Wintle (2000), Luminescence dating of quartz using an improved single-aliquot regenerative-dose protocol, *Radiat. Meas.*, *32*, 57–73, doi:10.1016/S1350-4487(99)00253-X.

Prescott, J. R., and J. T. Hutton (1994), Cosmic ray contributions to dose rates for luminescence and ESR dating: Large depths and long-term time variations, *Radiat. Meas.*, *23*, 497–500, doi:10.1016/1350-4487(94)90086-8.

Readhead, M. L. (2002), Absorbed dose fraction for [87]Rb β particles, *Ancient TL*, *20*, 25–27.

Reimer, P. J., et al. (2004), IntCal04 terrestrial radiocarbon age calibration, 0–26 cal kyr BP, *Radiocarbon*, *46*, 1029–1058.

Spooner, N. A. (1992), Optical dating: Preliminary results on the anomalous fading of luminescence from feldspars, *Quat. Sci. Rev.*, *11*, 139–145, doi:10.1016/0277-3791(92)90055-D.

Spooner, N. A. (1994), The anomalous fading of infrared-stimulated luminescence from feldspars, *Radiat. Meas.*, *23*, 625–632, doi:10.1016/1350-4487(94)90111-2.

Sun, J. M. (2000), Origin of eolian sand mobilization during the past 2300 years in the Mu Us Desert, China, *Quat. Res.*, *53*, 78–88, doi:10.1006/qres.1999.2105.

Sun, J. M., G. M. Yin, Z. L. Ding, T. S. Liu, and J. Chen (1998), Thermoluminescence chronology of sand profiles in the Mu Us Desert, China, *Palaeogeogr. Palaeoclimatol. Palaeoecol.*, *144*, 225–233, doi:10.1016/S0031-0182(98)00082-0.

Sun, J. M., Z. L. Ding, T. S. Liu, D. Rokosh, and N. Rutter (1999), 580,000-year environmental reconstruction from aeolian deposits at the Mu Us Desert margin, China, *Quat. Sci. Rev.*, *18*, 1351–1364, doi:10.1016/S0277-3791(98)00086-9.

Thompson, W. G., and S. L. Goldstein (2006), A radiometric calibration of the SPECMAP timescale, *Quat. Sci. Rev.*, *25*, 3207–3215, doi:10.1016/j.quascirev.2006.02.007.

Van Heteren, S., D. J. Huntley, O. van de Plassche, and R. K. Lubberts (2000), Optical dating of dune sand for the study of sea-level change, *Geology*, *28*, 411–414, doi:10.1130/0091-7613(2000)28<411:ODODSF>2.0.CO;2.

Voelker, A. H. L. (2002), Global distribution of centennial-scale records for Marine Isotope Stage (MIS) 3: A database, *Quat. Sci. Rev.*, *21*, 1185–1212, doi:10.1016/S0277-3791(01)00139-1.

Wallinga, J., A. S. Murray, G. A. T. Duller, and T. E. Tornqvist (2001), Testing optically stimulated luminescence dating of sand-sized quartz and feldspar from fluvial deposits, *Earth Planet. Sci. Lett.*, *193*, 617–630, doi:10.1016/S0012-821X(01)00526-X.

Wallinga, J., A. J. J. Bos, P. Dorenbos, A. S. Murray, and J. Schokker (2007), A test case for anomalous fading correction in IRSL dating, *Quat. Geochronol.*, *2*, 216–221, doi:10.1016/j.quageo.2006.05.014.

Wintle, A. G. (1973), Anomalous fading of thermoluminescence in mineral samples, *Nature*, *245*, 143–144, doi:10.1038/245143a0.

Wolfe, S. A., J. Ollerhead, D. J. Huntley, and O. B. Lian (2006), Holocene dune activity and environmental change in the prairie parkland and boreal forest, central Saskatchewan, Canada, *Holocene*, *16*, 17–29, doi:10.1191/0959683606hl903rp.

Zhao, H., and S. H. Li (2002), Luminescence isochron dating: A new approach using different grain sizes, *Radiat. Prot. Dosim.*, *101*, 333–338.

Zhao, H., and S. H. Li (2005), Internal dose rate to K-feldspar grains from radioactive elements other than potassium, *Radiat. Meas.*, *40*, 84–93, doi:10.1016/j.radmeas.2004.11.004.

————————

B. Li and S.-H. Li, Department of Earth Sciences, The University of Hong Kong, Room 309, James Lee Building, Pokfulam Road, Hong Kong 999077. (shli@hku.hk)

A. G. Wintle, Institute of Geography and Earth Sciences, University of Wales Aberystwyth, Llandinam Building, Penglais Campus, Aberystwyth SY23 3DB, UK.

H. Zhao, Key Laboratory of Desert and Desertification, Cold and Arid Regions Environment and Engineering Research Institute, Chinese Academy of Sciences, 320 Donggang West Road, Lanzhou 730000, China.